Biol. Chem., Vol. 389, pp. 623–632, June 2008 • Copyright © by Walter de Gruyter • Berlin • New York. DOI 10.1515/BC.2008.075

Review

Structures and specificity of the human kallikrein-related peptidases KLK 4, 5, 6, and 7

Mekdes Debela[1,2], Nathalie Beaufort[2], Viktor Magdolen[2], Norman M. Schechter[3], Charles S. Craik[4], Manfred Schmitt[2], Wolfram Bode[1] and Peter Goettig[1,*]

[1] Max-Planck-Institut für Biochemie, Proteinase Research Group, Am Klopferspitz 18, D-82152 Martinsried, Germany

[2] Klinische Forschergruppe der Frauenklinik, Klinikum rechts der Isar der TU München, Ismaninger Str. 22, D-81675 München, Germany

[3] Department of Dermatology, University of Pennsylvania, 415 Curie Blvd, Philadelphia, PA 19104, USA

[4] Department of Pharmaceutical Chemistry, University of California, 600 16th Street, San Francisco, CA 94143, USA

* Corresponding author
e-mail: goettig@biochem.mpg.de

Abstract

Human kallikrein-related peptidases (KLKs) are (chymo)-trypsin-like serine proteinases that are expressed in a variety of tissues such as prostate, ovary, breast, testis, brain, and skin. Although their physiological functions have been only partly elucidated, many of the KLKs appear to be useful prognostic cancer markers, showing distinct correlations between their expression levels and different stages of cancer. Recent advances in the purification of 'new type' recombinant KLKs allowed solution of the crystal structures of KLK4, KLK5, KLK6, and KLK7. Along with these data, enzyme kinetic studies and extended substrate specificity profiling have led to an understanding of the non-prime-side substrate preferences of KLK4, 5, 6, and 7. The shape and polarity of the specificity pockets S1–S4 explain well their substrate preferences. KLK4, 5, and 6 exhibit trypsin-like specificity, with a strong preference for Arg at the P1 position of substrates. In contrast, KLK7 displays a unique chymotrypsin-like specificity for Tyr, which is also preferred at P2. All four KLKs show little specificity for P3 residues and have a tendency to accept hydrophobic residues at P4. Interestingly, for KLK4, 5, and 7 extended charged surface regions were observed that most likely serve as exosites for physiological substrates.

Keywords: 99 loop; activation domain; inhibitors; substrate recognition.

Introduction: the KLK superfamily

Kallikrein-related peptidases, formerly named human tissue kallikreins (hKs), belong to a subgroup of the chymotrypsin-like serine proteinase family S1A of clan PA(S) (Yousef and Diamandis, 2001; Barrett et al., 2003; Clements et al., 2004). The 15 human KLK genes are located on chromosome 19q13.4 and constitute the largest contiguous serine protease cluster in the human genome (Yousef et al., 1999). These genes, generally composed of five coding exons and in some cases one or two 5′ non-coding exons, encode the classical tissue kallikrein KLK1 and the classical kallikrein-related peptidases KLK2 (glandular kallikrein) and KLK3 (prostate-specific antigen, PSA), as well as the 12 so-called new tissue kallikrein-related peptidases, KLK4–15, named in chronological order of their discovery (Brattsand and Egelrud, 1999; Yousef et al., 1999; Diamandis et al., 2000; Harvey et al., 2000; Yousef et al., 2000). All KLK genes encode single-chain pre-pro-proteinases containing a chymotrypsin- or trypsin-like catalytic domain of 224–237 residues (see Table 1 for details of KLK4–7) with an amino acid sequence identity of approximately 40% among the new members of the family (Clements et al., 2001; Yousef and Diamandis, 2002). According to phylogenetic analyses, KLK1 and its close homologs KLK2 and KLK3 form a clade of their own, KLK4, 5, and 7 belong to another subgroup, whereas KLK6 shares more similarities with KLK13 and KLK14 (Yousef and Diamandis, 2003; Clements et al., 2004). The 15 KLKs are secreted as inactive zymogens and are extracellularly activated by removal of their propeptides. The majority of these kallikrein-related peptidases prefer, like trypsin, basic P1 residues, whereas only a few members cleave similar to chymotrypsin or with a mixed chymo/trypsin-like P1 specificity (Debela et al., 2006b).

(Patho)physiological expression of kallikrein-related peptidases

The KLK proteinases are (co-)expressed within a wide range of tissues, such as the central nervous system, prostate, ovary, breast, testis, and skin (Shaw and Diamandis, 2007). According to this wide expression, KLK proteinases are involved, either directly or via participation in proteolytic cascades, in an array of physiological processes such as skin desquamation, neuronal plasticity, semen liquefaction, and tooth development (Simmer et al., 1998; Clements et al., 2001; Paliouras and Diamandis, 2006; Pampalakis and Sotiropoulou, 2007). Notably, KLK proteinase expression, which in many cases is under the control of steroid hormones, changes dramatically in a variety of malignant diseases (i.e., up- or

Table 1 General characteristics of KLK4, 5, 6, and 7.

	KLK4	KLK5	KLK6	KLK7
Other names	Prostase EM serine proteinase 1 Kallikrein-like protein 1 Serine protease 17	HSC tryptic enzyme Kallikrein-like protein 2	Protease M Neurosin Zyme Serine protease 9 Serine protease 18	HSC chymotryptic enzyme Serine protease 6
Protein length (aa)	254	293	244	253
Disulfide bonds (n)	6	6	6	6
N-Glycosylation sites	1	4	1	1
Signal peptide length (aa)	26	30	16	22
Pro-peptide length (aa)	4	37	5	7
Activation cleavage site	SCSQ-IING	SSSR-IING	EQNK-LVHG	QGDK-IIDG
Specificity	Trypsin-like	Trypsin-like	Trypsin-like	Chymotrypsin-like

EM, enamel matrix; HSC, human stratum corneum.

downregulated, depending on the type of cancer and KLK), with ovarian, breast, and prostate cancer being the most prominent examples (Borgono and Diamandis, 2004).

Like several other KLKs, KLK4, 5, 6, 7 are not or only moderately expressed in the normal ovary (Shaw and Diamandis, 2007), but are overexpressed in ovarian carcinoma tissues at the mRNA and/or protein level (Obiezu and Diamandis, 2005; Paliouras and Diamandis, 2007). High KLK4 and KLK5 mRNA levels are indicators of poor prognosis for ovarian cancer (Kim et al., 2001; Obiezu et al., 2001). Likewise, elevated KLK7 mRNA expression in tumor tissue is associated with poorer prognosis for ovarian cancer patients, especially for those with lower grade disease and those who have been optimally debulked (Kyriakopoulou et al., 2003). Ovarian cancer patients also express KLK6 protein in their tumor tissues, high levels of which are associated with shorter disease-free and overall survival (Hoffman et al., 2002). An *in vivo* tumor model demonstrated that simultaneous overexpression of KLK4, 5, 6, and 7 increases the malignant phenotype of ovarian cancer cells (Prezas et al., 2006). Thus, these enzymes may well be involved in ovarian tumor establishment, growth and/or spread, and should be considered as promising therapeutic targets.

In contrast to their general overexpression in ovarian cancer, KLK genes and proteins seem to be often downregulated in breast, prostate, and testicular tumors. Strikingly, whereas high KLK7 mRNA levels are significantly correlated with poorer prognosis of ovarian cancer patients (Kyriakopoulou et al., 2003), we observed that high KLK7 mRNA expression is strongly associated with good prognosis in breast cancer patients, indicating a different role of KLK7 in these two tumor types.

Aberrant KLK expression in tumor tissue may be due to DNA methylation, as recently reported for KLK6 in breast cancer (Pampalakis and Sotiropoulou, 2006). Moreover, a significant number of KLK splice variants have been identified, either resulting in premature stop of translation or the production of truncated non-functional proteinases. Several reports hint at a clinical significance for some of these novel KLK variants (Obiezu and Diamandis, 2000; Dong et al., 2003; Yousef et al., 2004; Kurlender et al., 2005; Tan et al., 2006). Apart from malignancies, KLKs are also involved in: (i) abnormal tooth development that is caused by the well-documented human autosomal recessive hypomaturation amelogenesis imperfecta, resulting from a KLK4 gene deletion (Hart et al., 2004); (ii) neurodegenerative disorders, e.g., KLK6 has been implicated in demyelinization processes (Blaber et al., 2004); and (iii) skin diseases, such as Netherton syndrome, for which unregulated KLK activity has been implicated in abnormal stratum corneum barrier function. Netherton syndrome has been genetically linked to a defect in the *SPINK5* gene, which encodes an inhibitor of KLK5 and 7, lymphoepithelial Kazal-type-related serine protease inhibitor (LEKTI) (Chavanas et al., 2000; Descargues et al., 2005).

Activation of kallikrein-related peptidases

Mature KLKs have a typical serine protease catalytic domain and lack other distinct domains such as growth factor-like or kringle domains found, for example, in serine proteases involved in clotting/fibrinoloysis. Since their biological function is likely to rely on their proteolytic activity only, major efforts have recently been made to elucidate pathways leading to KLK activation from precursor (zymogen) forms. All KLKs are synthesized as inactive pre-pro-enzymes and are translocated as inactive zymogens into the endoplasmic reticulum upon removal of the signal peptide. After secretion into the extracellular space, the pro-KLKs are activated by proteolytic release of a propeptide from the N-terminus, typically 4–9 aa in length. The exception is KLK5, which possesses an unusually long propeptide of 37 aa (Table 1). Because the KLK activation cleavage site bears a P1-Arg or a Lys residue, with the exception of Gln in pro-KLK4, KLK activation is likely to involve proteinases endowed with trypsin-like specificity. Since many KLK proteinases themselves have trypsin-like substrate specificity (Table 2), it has been proposed that KLKs are capable of activating themselves, each other, and co-expressed chymotrypsin-like KLKs, thereby producing an activity amplification cascade analogous to that observed for digestive enzymes, blood coagulation and the complement system, respectively (Bode et al., 1997; Gros et al., 2008). Such amplification of activity may generate the active enzymes to produce desquamation in the skin or semen liquefaction in the prostate (Pampalakis and Sotiropoulou, 2007).

Table 2 Selected potential natural substrates of KLK4, 5, 6, or 7 with a determined cleavage site.

Natural substrate	Cleavage site	References
KLK4		
Pro-urokinase	PRFK-IIGG*	1, 2
Pro-meprin β	AQIR-NSII*	3
Pro-KLK3	ILSR-IVGG*	1
Pro-KLK11	GETR-IIGK*	4, 5
Prostatic acid phosphatase	VYIR-STDV	1
Urokinase receptor	AVTY-SRSR	2
	TYSR-SRYL	2
	VQYR-SG	2
Enamelin	VPHR-IPPG	6
	FFGY-HGFG	6
	FGYH-GFGG	6
	SEEM-FEQD	6
	PNPR-GNDT	6
Amelogenin	LTPL-KWYQ	7
	TPLK-WYQN	7
	LKWY-QNMI	7
	NMIR-HPYT	7
	WLHH-QIIP	7
	PQSH-ALQP	7
	PLPA-QQPF	7
	FSMQ-SLLP	7
KLK5		
Pro-uPA	PRFK-IIGG*	5
Plasminogen	LFEK-KVYL	8
	TNPR-KLYD	8
Pro-meprin α	QKSR-NGLR	9
Pro-meprin β	AQIR-NSII*	9
Kininogen	IQLR-IASF	8
	GCPR-DIPT	8
	RSSR-IGEI	8
Pro-KLK2	IQSR-IVGG*	10
	LRPR-SLQC	10
Pro-KLK3	ILSR-IVGG*	10
	LKNR-FLRP	10
	TGGK-STCS	10
Pro-KLK5	SSSR-IING*	11
Pro-KLK6	EQNK-LVHG*	12
Pro-KLK7	QGDK-IIDG*	11
Pro-KLK11	GETR-IIGK*	4, 5
Pro-KLK12	ATPK-IFNG*	4
Pro-KLK14	DENK-IIGG*	12
Protease-activated receptor 2	SKGR-SLIG*	13, 14, 15
Cathelicidin	KRFA-LLGD*	16
	DFRR-KSKE	16
	DFLR-NLVP	16
	EFKR-IVQR	16
	IVQR-IKDF	16
	LVPR-TES	16
Fibrinogen (α-chain)	SSER-GSAG	8
	GTRR-EYHT	8
Fibrinogen (β-chain)	FSAR-GHRP	8
	ATQK-KVER	8
Vitronectin	CKGR-CTEG	8
IGFBP-1	DGSK-ALHV	10
IGFBP-2	EQHR-QMGK	10
IGFBP-3	DSQR-YKVD	10
	LSPR-GVHI	10
IGFBP-4	SQSR-THED	10
IGFBP-5	KHTR-ISEL	10
	MVPR-AVYL	10
KLK6		
Pro-urokinase	PRFK-IIGG*	5
Pro-KLK6	LRQR-ESSQ	12, 17, 18
Pro-KLK11	GETR-IIGK*	4
Plasminogen	LFEK-KVYL	18
	FEKK-VYLS	18
	TEAS-VVAP	18
Protease-activated receptor 2	SKGR-SLIG*	13, 14
Myelin basic protein	SQKR-PSQR	19
	PSQR-HATA	19
	DHAR-HGFL	19
	FLPR-HRDT	19
	PRHR-DTGI	19
	SIGR-FFGG	19
	GGDR-GAPK	19
	APKR-GSGK	19
	HPAR-TAHY	19
	LPQK-SHGR	19
	SHGR-TQDE	19
	HFFK-NIVT	19
	VTPR-TPPP	19
	GKGR-GLSL	19
	SLSR-FSWG	19
	YGGR-ASDY	19
Amyloid precursor protein	SEVK-MDAE	17, 19
	AEFR-HDSG	17, 19
	HHQK-LVFF	17, 19
KLK7		
Cathelicidin	GKEF-KRIV	16
	GDFF-RKSK	16
	LGDF-FRKS	16
	IKDF-LRNL	16
Insulin B-chain	NQHL-CGSH	20
	EALY-LVCG	20
	RGFF-YTPK	20
	GFFY-TPKT	20

*Activation of the target protein. IGFBP: insulin-like growth factor-binding protein. References: (1) Takayama et al., 2001; (2) Beaufort et al., 2006; (3) Becker-Pauly et al., 2007; (4) Yoon et al., 2007; (5) our unpublished results; (6) Yamakoshi et al., 2006; (7) Hart et al., 2004; (8) Michael et al., 2005; (9) Becker-Pauly et al., personal communication; (10) Michael et al., 2006; (11) Brattsand et al., 2005; (12) Blaber et al., 2007; (13) Oikonomopoulou et al., 2006a; (14) Oikonomopoulou et al., 2006b; (15) Stefansson et al., 2008; (16) Yamasaki et al., 2006; (17) Magklara et al., 2003; (18) Bayés et al., 2004; (19) Angelo et al., 2006; (20) Skytt et al., 1995.

Accordingly, MMP-20 might activate KLK4 (Simmer and Hu, 2002) and it has been shown that KLK4 is capable of processing the zymogens of several KLKs, including KLK3, and 11, into their active counterparts (Takayama et al., 2001; Yoon et al., 2007; our unpublished results), although *in vivo*, or at least *ex vivo,* demonstrations are still lacking. Evidence also indicates that (pro-)KLK5 is capable of auto-activation and that this enzyme could then activate pro-KLK2, 3, 6, 7, 11, 12 and 14 (Brattsand et al., 2005; Michael et al., 2006; Blaber et al., 2007; Yoon et al., 2007; our unpublished results). KLK4 and 5 may therefore be considered general activators of pro-KLKs. KLK6, whose pro-fragment is removed by treatment with KLK5, activates mainly pro-KLK11 (Yoon et al., 2007). To date it has not been clearly demonstrated that KLK7, a chymotrypsin-like protease, activates pro-forms of other KLKs, although it has the capacity to cleave the propeptides of KLK2 and 3,

despite an Arg in P1 position (Yoon et al., 2007). Interestingly, KLKs also exhibit internal peptide bonds that are sensitive to trypsin-like protease cleavage, which results in inactivation. Therefore, in some cases activation is only a transitional step that is rapidly followed by autoproteolytic inactivation of the KLK enzyme, as in the case of KLK6 via cleavage of the internal Arg76-Glu77 peptide bond (Magklara et al., 2003; Bayés et al., 2004; Blaber et al., 2007). Such autoproteolytic cleavage, which is not generally observed after activation of other serine proteases, may be an important feature for regulation of the activity of various KLKs, along with their known sensitivity to an array of natural protease inhibitors, including α_2-macroglobulin, serpins and/or LEKTI, and salts, e.g., Zn^{2+} and Cu^{2+} ions.

Structural and functional comparison of KLK4, 5, 6, and 7

In addition to the classical kallikreins, KLK1 (1SPJ; Laxmikanthan et al., 2005) and KLK3 (2CZH; Menez et al., 2008), crystal structure coordinates of mature new type human kallikrein-related peptidases are available for recombinant KLK4 (2BDG; Debela et al., 2006a), KLK5 (2PSX; Debela et al., 2007a), KLK6 (1LO6; Bernett et al., 2002), and KLK7 (2QXH; Debela et al., 2007b). All four kallikrein-related peptidases are shaped like an oblate ellipsoid with diameters of approximately 35 and 50 Å. Similar to other trypsin-like serine proteinases, the chain folds into two adjacent six-stranded β-barrels that are tightly interconnected by three trans-domain segments. The typical structure includes one 3_{10}-helix between residues 55 and 59 and two α-helices in segments 164–172 and 234–244. KLK4 also contains a short 3_{10}-helix between residues 74 and 77 in the 75 (70–80) loop (Debela et al., 2006a). The catalytic triad of Ser195, His57, and Asp102 is located along the junction of both barrels, and the active-site cleft with the substrate recognition subsites S4–S3′ runs perpendicular to this junction (Figure 1A). Consistent with most other trypsin-like protease structures is the presence of an internal salt bridge between the α-ammonium group of Ile/Leu16 and the side-chain carboxylate of Asp194. Formation of this buried salt bridge is the basis for zymogen activation, as its presence confers rigidity to the overall structure of the protease and maintains the S1 pocket in the correct conformation to bind substrates and to stabilize transition-state intermediates through the oxyanion hole, which consists of the backbone amides of Ser195 and Gly193 (Bode et al., 1978; Huber and Bode, 1978) (Figure 1). The two major specificity-determining residues Asp(Asn)189 and the adjacent Ser(Ala)190 are located at the bottom of the S1 pocket (Figure 1B).

Further common characteristics are the presence of *cis*-Pro219 (a residue that is deleted in human trypsin, thrombin, and tryptases), Pro225, which prevents sodium binding in the 222 loop, as observed in coagulation factors (Di Cera et al., 1997), and six disulfide bridges (Cys22-Cys157, Cys42-Cys58, Cys128-Cys232, Cys136-Cys201, Cys168-Cys182 and Cys191-Cys220). Noteworthy is the sequence variation in the 37 loop of KLK5 that is one residue longer than those of KLK4, 6, and 7. The 70–80 loop of KLK4 and KLK5 contains the

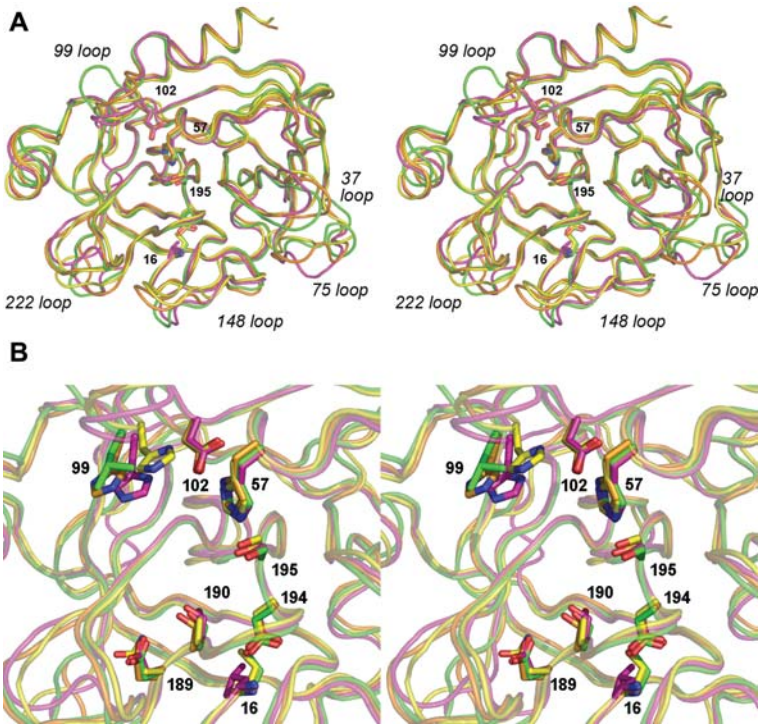

Figure 1 Superposition of the kallikrein-related peptidase KLK4, 5, 6, and 7 tertiary structures in standard orientation.
(A) Overall structures depicted as coils for all secondary structural elements in stereo. KLK4 is displayed in green, KLK5 in orange, KLK6 in magenta, and KLK7 in yellow. Important loops are labeled according to their middle residues. The catalytic triad residues Ser195, His57, Asp102, and the N-terminal residue 16 are shown as stick models. (B) Close-up view of the active sites in the same orientation as in (A), with additional stick models for residues 99, 189, and 190.

inserted residue 74A with respect to the chymotrypsinogen numbering, whereas KLK7 exhibits a two-residue deletion. The 99 loop of all four KLKs is exactly the same length as in chymotrypsinogen and lacks the so-called kallikrein-loop, an 11-residue insertion in the 99 loop present in the classical kallikreins KLK1–3 (Clements et al., 2001). Furthermore, the 148 loops of KLK4 and KLK6 have a two-residue deletion compared to those of KLK5, KLK7, and chymotrypsinogen. With the exception of a single-residue deletion after residue 186, the sequence numbering of these four KLKs does not differ any further. Using KLK4 as the reference structure (Figure 1) superimposition of the other KLKs resulted in root mean square (rms) deviations of 0.83 Å for KLK5 (54.5% identical residues), 0.88 Å for KLK6 (43.8%), and 1.04 Å for KLK7 (50.7%).

The extended substrate specificity has been investigated for KLK4 (Matsumura et al., 2005; Debela et al., 2006b; Borgoño et al., 2007), KLK5 (Michael et al., 2005; Debela et al., 2006b; Borgoño et al., 2007), KLK6 and KLK7 (Debela et al., 2006b). Owing to the more open, hydrophobic character of the S4 subsite (Schechter and Berger, 1967), all investigated human KLKs are rather non-specific for P4 residues, with a slight preference for hydrophobic residues. The S3 subsite also shows little specificity, as the P3 side chains mostly extend to the bulk solvent (Debela et al., 2006b). Therefore, only the S1 and S2 subsite of KLK4, 5, 6, and 7 are discussed here in detail. In addition, the primed subsites S1′, S2′ or even further have not been characterized systematically for the KLKs. Based on crystal structures and comparison of cleavage sites within biological proteins, this portion of the extended substrate binding site might favor small to medium-sized polar or hydrophobic residues.

KLK4

KLK4 (hK4) has a clear preference for P1-Arg over Lys side chains in its S1 specificity pocket, which also tolerates Gly, Gln, and Asn, according to two positional scanning studies (Matsumura et al., 2005; Debela et al., 2006b) and a kinetic study using tripeptidyl-*p*-nitro-anilides (pNA) with P1-Arg and P1-Lys (Takayama et al., 2001). Furthermore, KLK4 prefers as P2 residue the medium-sized polar Gln over the more hydrophobic Val, Leu, Thr, and Pro, whereas large aromatic and basic side chains are not accepted (Debela et al., 2006b). Among the four kallikrein-related peptidases being discussed, KLK4 is the only one that has marked specificity for medium-sized to large hydrophobic P4 residues. The catalytic efficiency of KLK4 for the hydrolysis of Z-FVR-pNA was exceptionally high, demonstrating a k_{cat}/K_m value of 1.75×10^6 M^{-1} s^{-1} (Debela et al., 2006a).

Some efficient *in vitro* substrates of KLK4 (Table 2) have cleavage sites that correspond to the profiling results (Wright et al., 2003; Yamakoshi et al., 2006; Becker-Pauly et al., 2007), such as the proform of KLK3 with the Ile-Leu-Ser-Arg-↓-Ile-Val activation site. KLK4 also activates the urokinase-type plasminogen activator (uPA) by cleaving after Pro-Arg-Phe-Lys (Takayama et al., 2001) and cleaves the uPA receptor (uPAR) after Thr-Tyr-Ser-Arg, as well as in the sequence Val-Gln-Tyr-Arg-↓-Ser-Gly (Beaufort et al., 2006). Therefore, it is assumed that KLK4 might be a physiological regulator of these cancer-associated enzymes.

Overall, these functions are in good agreement with the structural characteristics of the KLK4 active site. In the crystal structure of KLK4, a *p*-amino benzamidine (PABA) inhibitor molecule is bound in the large and deep S1 pocket. Owing to the presence of an amidino group, the binding of PABA most closely resembles the interaction of the S1 subsite with a P1-Arg (Figure 2A). In the crystal structure, the positively charged amidino group forms a salt bridge to the negatively charged Asp189 carboxylate at the very bottom of the S1 pocket (two O-two N hydrogen bonds), and a hydrogen bond to the adjacent polar Ser190 Oγ, which most likely supports the accommodation of P1-Lys side chains (Debela et al., 2006a). Additional hydrogen bonds of the PABA amidino group were observed with a buried water molecule and with the backbone carbonyl of Lys217. The S2 subsite of KLK4 is a uniquely notched S2 groove, well shaped to accept medium-sized hydrophobic and polar P2-side chains (Figure 2A). It is largely constituted by the side chains of His57, Leu99, and Phe215, but is more deeply carved than in KLK5, 6, and 7 (Figure 1B). Moreover, it has more negative potential, because the Asp102 side chain is only partially shielded from the bulk solvent (Figure 2A). The hydrophobic S4 cleft of KLK4 is also better defined than those of KLK5, 6, and 7 by the Phe215 phenyl side chain and by the bordering Leu175 and Leu99, and can accommodate medium-sized to large hydrophobic P4 side chains.

KLK5

Among the kallikrein-related peptidases investigated, KLK5 (hK5) or human stratum corneum trypsin-like enzyme (Brattsand and Egelrud, 1999) exhibits the strongest preference for P1-Arg over Lys and the complete exclusion of chymotrypsin-specific substrates with a Phe or Tyr side chain in P1 position (Michael et al., 2005; Debela et al., 2006b). Since KLK5 activates pro-KLK7 (Gln-Gly-Asp-Lys-↓-Ile-Ile) at a low rate (Caubet et al., 2004), Lys is accepted by the S1 pocket to some extent. In a comparative study using fluorogenic tripeptidyl substrates, a preference for Ala and Lys at P2 was identified; however, the best substrates were the 7-amino-4-methyl coumarins (AMC) of Boc-Phe-Ser-Arg and Boc-Val-Pro-Arg, which had k_{cat}/K_m values around 15×10^3 M^{-1} s^{-1} (Michael et al., 2005). Relative to KLK4, model peptide pNA substrates were hydrolyzed with much less efficiency by KLK5, e.g., Bz-Pro-Phe-Arg-pNA exhibited k_{cat}/K_m of 6.60×10^3 M^{-1} s^{-1} (Schechter et al., 2005). A recent profiling study demonstrated that small or polar residues are preferred in P2, such as Ser, Ala, Thr, and Asn (Debela et al., 2006b). However, KLK5 activates itself more efficiently at the cleavage site Ser-Ser-Ser-Arg-↓-Ile-Ile than KLK7 or KLK14, which, together with KLK8 and KLK6, may interact in a proteolytic cascade of the stratum corneum, serving in skin desquamation (Brattsand et al., 2005; Pampalakis and

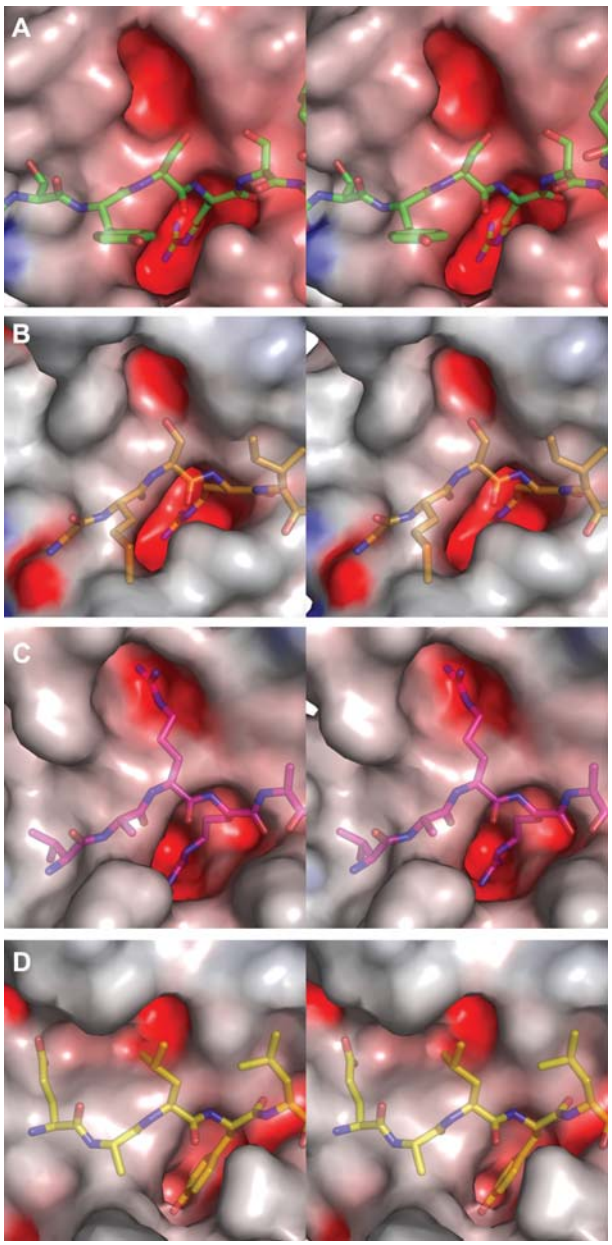

Figure 2 Stereo representation of the unprimed substrate-binding site region of KLK4, 5, 6, and 7 in standard orientation. (A) Active-site cleft of KLK4 in electrostatic surface representation with the modeled substrate Thr-Tyr-Ser-Arg-↓-Ser-Arg depicted as a stick model. (B) Active site of KLK5 in electrostatic surface representation with the modeled substrate Gly-Met-Ser-Arg-↓-Ile-Ile shown as a stick model. (C) Active-site cleft of KLK6 in electrostatic surface representation with the modeled substrate Val-Ala-Arg-Arg-↓-Ala-Ala displayed as a stick model. (D) Active site of KLK7 in electrostatic surface representation with the modeled substrate Glu-Ala-Leu-Tyr-↓-Leu-Val depicted as a stick model.

Sotiropoulou, 2007) and immune defense (Yamasaki et al., 2006). Optimal substrate sequences for KLK5 were derived from the N-terminal propeptide of KLK3 Ile-Leu-Ser-Arg-↓-Ile-Val (Michael et al., 2006), which is in accordance with the scanning library results (Debela et al., 2006b), in which an unusual preference for Gly in P4 was observed. Although their cleavage sites have not been characterized in detail, several protein components of corneodesmosomes, adhesion structures that connect corneocytes in the outermost layers of human skin, have been found to be good substrates of KLK5 (Caubet et al., 2004). As also shown for KLK6 and KLK14 (but not for KLK7 and KLK8), KLK5 is able to induce signaling events via proteinase-activated receptor-2 (PAR2; Oikonomopoulou et al., 2006a,b; Stefansson et al., 2008), a seven-transmembrane G protein-coupled receptor present on the membrane of many cell types, including keratinocytes (Table 2).

The leupeptin inhibitor (Ac-Leu-Leu-Arg-HC=O) bound in the KLK5 crystal structure resembles a tripeptide occupying the unprimed subsite region, with the N-terminal methyl group of the acetyl located in the S4 subsite (Debela et al., 2007a). As in an ideal substrate (Figure 2B), the P1-Arg side chain reaches the bottom of the deep S1 pocket and forms a stabilizing salt bridge between its positively charged guanidyl group and the carboxylate group of Asp189. In addition, hydrogen bonds are formed to the Ser190 Oγ, to a buried water molecule, and to the carbonyl group of Asp217. However, the strong preference of KLK5 for P1-Arg over Lys cannot directly be explained by its structural components. The S2 subsite of KLK5 is a wedge-shaped pocket mainly formed by the side chains of His99 and His57 (Figures 1B, 2B). It is not as deep as the S2 subsite of KLK4 and is more polar in character. The accommodation of a medium-sized hydrophobic side chain such as the P2 Leu of leupeptin requires some rotation of His99.

KLK6

KLK6, like KLK4, displays a marked preference for P1-Arg over Lys (Debela et al., 2006b). However, both proteases differ in that Ala and Met are slightly more preferred KLK6 P1 residues than Lys, suggesting that the S1 subsite has some chymotrypsin-like specificity (Debela et al., 2006b). The high specificity of KLK6 for P1-Arg is in accordance with the efficient turnover of fluorescent Xaa-Xaa-Arg-AMC substrates in enzyme assays (Yamaguchi, 2004). Interestingly, the S2 subsite of KLK6 is the most selective among the KLKs tested in a positional scanning study, and exhibited an unusually strong specificity for Arg and Lys at the P2 position of substrates (Debela et al., 2006b). The catalytic efficiency of KLK6 for the hydrolysis of model peptide substrates appears to be in the same low range as that of KLK5, as observed for the fluorogenic substrate Tos-Gly-Pro-ARG-AMC, with k_{cat}/K_m of 4.40×10^3 M^{-1} s^{-1}. Potential natural substrates of KLK6, such as the human ionotropic glutamate receptors (iGluR) and the myelin basic protein (MBP), were the basis for the synthesis of good *in vitro* substrates with the motifs Ala-Phe-Arg-↓-Phe-Ser or His-Pro-Ala-Arg-↓-Thr-Ala (Angelo et al., 2006) (Table 2).

As in the KLK4 crystal structure, a benzamidine molecule was bound in the S1 site of KLK6, mimicking a P1-Arg (Bernett et al., 2002). The depth and size of the KLK6 S1 pocket (Figure 2C) resemble those of KLK4 (Debela et al., 2006a), KLK5 (Debela et al., 2007a), and bovine trypsin (Bode and Schwager, 1975). The negatively charged Asp189 side chain at the bottom of the pocket explains the specificity for basic P1 residues, whereas the Ser190 side chain supports the acceptance of Lys side chains. The architecture of the S2 pocket of KLK6

is similar to the wedge-shaped pocket of KLK5, being formed by imidazole groups of His99 and His57 (Figure 1B) with a significant negative electrostatic potential that is mostly generated by Asp102. However, the S2 pocket of KLK6 is more carved out than in KLK5 (Figure 2B,C) and is more open than in KLK4 (Figure 2A), and could adapt to larger substrates by a corresponding side chain rotation, as observed for the equivalent Tyr99 side chain of porcine kallikrein 1 (pK1) complexed with BPTI (Chen and Bode, 1983). Thus, the P2-Arg and P2-Lys preference of KLK6 is mainly explained by the favorable steric situation in combination with the negative potential of Asp102.

KLK7

According to specificity profiling, the most preferred P1 residue of KLK7 is Tyr, followed by Ala and Met, whereas Phe, Arg, and Lys are ranked quite low (Debela et al., 2006b). Interestingly, Tyr is favored at S2 over the medium-sized hydrophobic residues Leu, Thr, Met, and Phe. In agreement with these findings, KLK7 cleaves the insulin B-chain after Asn-Gln-His-Leu, Glu-Ala-Leu-Tyr, Gly-Phe-Phe-Tyr, and Arg-Gly-Phe-Phe (Skytt et al., 1995; Egelrud, 2004) (Table 2). A slow turnover of substrates with Phe in the P1 position has been reported, e.g., Suc-Ala-Val-Pro-Phe-pNA, a substrate usually hydrolyzed with high efficiency ($k_{cat}/K_m > 10^5$ M^{-1} s^{-1}) by chymotrypsin-like proteases (Powers et al., 1985), demonstrated a very low k_{cat}/K_m of 16.0 M^{-1} s^{-1} (Schechter et al., 2005). Similar to KLK5, KLK7 degrades proteins of corneodesmosomes, which are most likely physiological substrates of KLKs expressed in the stratum corneum of skin (Caubet et al., 2004). KLK7 also degrades human lipid-processing enzymes, such as β-glucocerebrosidase and acidic sphingomyelinase, which produce ceramide-type lipids deposited in the stratum corneum (Hachem et al., 2005).

Recently, two crystal structures of KLK7 have been solved with either of two covalently bound chloromethyl ketone (CMK) inhibitors, Ala-Ala-Phe-CMK and Suc-Ala-Ala-Pro-Phe-CMK, bound within the active site (Debela et al., 2007b). Overall, the S1 pocket of KLK7 is larger and more hydrophobic than those of the tryptic KLK4, 5, and 6 (Figure 2D). The hydrophobicity of the S1 pocket is enhanced by the presence of Ala190 instead of Ser190, and at the bottom of the pocket, Asn189, a polar residue, replaces Asp189, a negatively charged residue (Figure 1B). Consistent with specificity, Asn189 instead of Asp189 would reduce the affinity of KLK7 for basic P1 side chains and allow binding of non-polar residues. The size and shape of the S1 pocket is well suited to accommodate residues with medium and large side chains, explaining the modified chymotryptic specificity. Tyr may be favored over Phe at P1 because of the potential of the carboxyamide group of Asn189 to hydrogen bond to a buried hydroxyl group (Figure 2D). Owing to the conformational restrictions of the relatively narrow S1 pocket, the formation of a stabilizing hydrogen bond between the P1-Tyr-OH and the carboxamide of Asn189 has to be mediated by a water molecule (Debela et al., 2007b). The S2 subsite is less separated from the S4 subsite than in KLK4–6 and less limited in size owing to a different position of the His99 imidazole side chain (Figure 1B), which may also contribute to the capacity for the adaptation to P2 side chains of various size. Nevertheless, the S2 pocket exhibits some specificity for medium-sized polar and hydrophobic residues, such as Tyr, Leu, Met, and Thr.

Conclusions

We have compared three kallikrein-related peptidases with tryptic specificity (KLK4, 5, and 6) and one with modified chymotryptic specificity (KLK7) based on their substrate preferences, kinetic data, and crystal structures

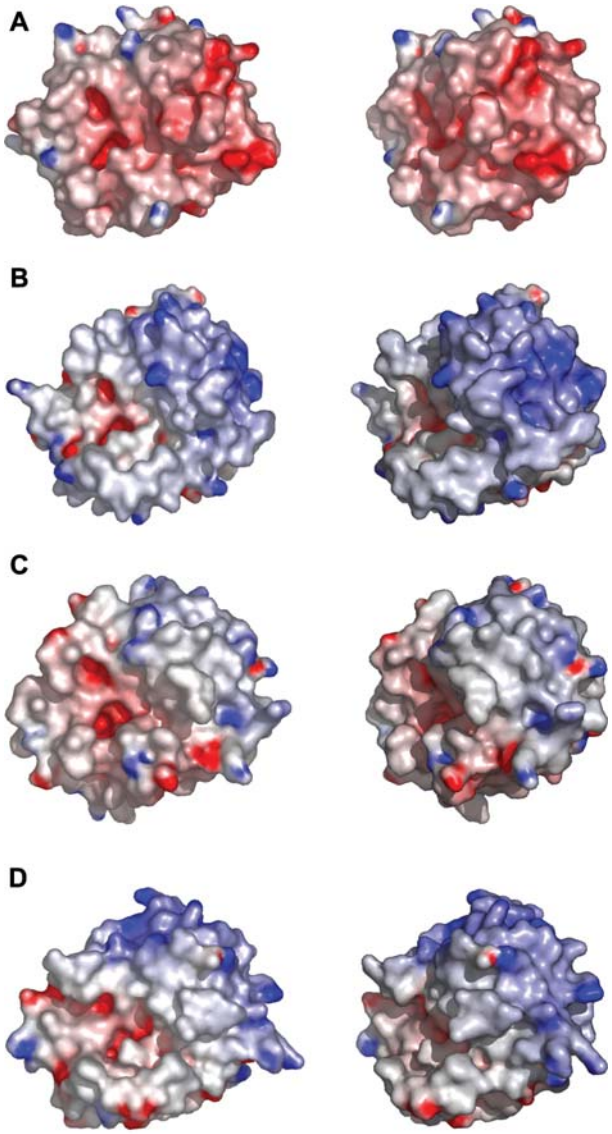

Figure 3 Molecular surface representation with electrostatic potentials for KLK4–7 focusing on the putative exosites for substrate recognition.
In the panels on the left, KLK molecules are displayed in standard orientation as in Figure 1, while they are rotated by 30° in the panels on the right. (A) KLK4 exhibits a negatively charged patch close to the primed side region. (B) KLK5 possesses a large positively charged region between the primed side and its C-terminus. (C) KLK6 has an even charge distribution in this region. (D) KLK7 possesses a positively charged region similar to KLK5.

with bound inhibitor molecules. Since these KLKs belong to the subgroup of new tissue kallikreins that lack the 11-residue insert in the 99 loop, their unprimed substrate recognition region is relatively similar. Whereas the specificity in S4 for hydrophobic residues follows the order KLK4>KLK5>KLK6>KLK7 (non-specific), the S3 subsite is non-specific in general. The S2 pocket of KLK6 is the most specific, with a strong preference for basic side chains, whereas KLK5 prefers more polar P2 side chains, KLK4 rejects charged and large residues, and KLK7 favors medium-sized polar and hydrophobic residues. Seemingly, the major determinant of specificity for KLK4–7 is the S1 pocket. Among the three tryptic KLKs, the following order for specificity is observed: KLK5>KLK4>KLK6. The latter displays an increased chymotryptic component in its substrate preference. Finally, KLK7 possesses a unique modified chymotryptic specificity, with an unusual preference for Tyr.

Further determinants of substrate recognition and specificity for physiological polypeptide substrates may be found in the novel exosites of KLK4, 5, and 7, which have no counterpart in KLK6 (Figure 3). Adjacent to the primed subsites of KLK4 extends a negatively charged region around the 37 loop and the 75 loop with the center Glu84 (Debela et al., 2006a). Remarkably, this exosite coincides with the positively charged anion-binding exosite I of thrombin, which is involved in various substrate and inhibitor interactions (Bode et al., 1989) (Figure 3A). Both KLK5 (Debela et al., 2007a) and KLK7 (Debela et al., 2007b) exhibit similar positively charged exosites that extend even further to the C-terminal helix (Figure 3B,D). Usually, such exosites enhance the efficiency of cleavage, which otherwise can be very low for small test substrates, as observed for KLK7 (Schechter et al., 2005; Debela et al., 2007b), or allow for the turnover of non-optimal cleavage sequences in physiological substrates. However, the identification of endogenous KLK substrates by structural and specificity profiling data should be supported by considering interaction with potential exosites and cofactors, in particular bivalent cations.

Zinc inhibition in the low μM concentration range was observed for several kallikrein-related peptidases, among them KLK4 (Debela et al., 2006a), KLK5 (Michael et al., 2006), and KLK7 (Debela et al., 2007b). In addition, metal-binding sites that are responsible for the inhibitory Zn^{2+} effect have been identified in the crystal structures (Debela et al., 2006a, 2007a,b). However, the corresponding physiological role of Zn^{2+} and its influence on substrate recognition and turnover require further studies. Certainly, for the development of highly specific drugs such as active site inhibitors, a detailed understanding of the mode of action of theses serine proteinase is required that is based not only on their three-dimensional structures and knowledge of their extended substrate specificity beyond the scissile bond residues, but also on the fine-tuned regulation of their activity under physiological conditions.

Acknowledgments

We are grateful to Robert Huber and Reinhard Fässler for continuous support. Financial support by the European Commission through SPINE contract no. QLG2-CT-2002-00988 under the integrated program 'Quality of Life and Management of Living Resources' and project CAMP LSHG-2006-018830, by Fonds der Chemischen Industrie to Wolfram Bode, by Bayerische Forschungsstiftung and Alexander von Humboldt Foundation to Nathalie Beaufort and Viktor Magdolen, by Graduiertenkolleg 333 of Deutsche Forschungsgemeinschaft to Mekdes Debela and Viktor Magdolen, and by National Institutes of Health grant CA072006 to Charles S. Craik is kindly acknowledged.

References

Angelo, P.F., Lima, A.R., Alves, F.M., Blaber, S.I., Scarisbrick, I.A., Blaber, M., Juliano, L., and Juliano, M.A. (2006). Substrate specificity of human kallikrein 6: salt and glycosaminoglycan activation effects. J. Biol. Chem. *281*, 3116–3126.

Barrett, A.J., Tolle, D.P., and Rawlings, N.D. (2003). Managing peptidases in the genomic era. Biol. Chem. *384*, 873–882.

Bayés, A., Tsetsenis, T., Ventura, S., Vendrell, J., Aviles, F.X., and Sotiropoulou, G. (2004). Human kallikrein 6 activity is regulated via an autoproteolytic mechanism of activation/inactivation. Biol. Chem. *385*, 517–524.

Beaufort, N., Debela, M., Creutzburg, S., Kellermann, J., Bode, W., Schmitt, M., Pidard, D., and Magdolen, V. (2006). Interplay of human tissue kallikrein 4 (hK4) with the plasminogen activation system: hK4 regulates the structure and functions of the urokinase-type plasminogen activator receptor (uPAR). Biol. Chem. *387*, 217–222.

Becker-Pauly, C., Howel, M., Walker, T., Vlad, A., Aufenvenne, K., Oji, V., Lottaz, D., Sterchi, E.E., Debela, M., Magdolen, V., et al. (2007). The α and β subunits of the metalloprotease meprin are expressed in separate layers of human epidermis, revealing different functions in keratinocyte proliferation and differentiation. J. Invest. Dermatol. *127*, 1115–1125.

Bernett, M.J., Blaber, S.I., Scarisbrick, I.A., Dhanarajan, P., Thompson, S.M., and Blaber, M. (2002). Crystal structure and biochemical characterization of human kallikrein 6 reveals that a trypsin-like kallikrein is expressed in the central nervous system. J. Biol. Chem. *277*, 24562–24570.

Blaber, S.I., Ciric, B., Christophi, G.P., Bernett, M.J., Blaber, M., Rodriguez, M., and Scarisbrick, I.A. (2004). Targeting kallikrein 6 proteolysis attenuates CNS inflammatory disease. FASEB J. *18*, 920–922.

Blaber, S.I., Yoon, H., Scarisbrick, I.A., Juliano, M.A., and Blaber, M. (2007). The autolytic regulation of human kallikrein-related peptidase 6. Biochemistry *46*, 5209–5217.

Bode, W. and Schwager, P. (1975). The refined crystal structure of bovine β-trypsin at 1.8 Å resolution. II. Crystallographic refinement, calcium binding site, benzamidine binding site and active site at pH 7.0. J. Mol. Biol. *98*, 693–717.

Bode, W., Schwager, P., and Huber, R. (1978). The transition of bovine trypsinogen to a trypsin-like state upon strong ligand binding. The refined crystal structures of the bovine trypsinogen-pancreatic trypsin inhibitor complex and of its ternary complex with Ile-Val at 1.9 Å resolution. J. Mol. Biol. *118*, 99–112.

Bode, W., Mayr, I., Baumann, U., Huber, R., Stone, S.R., and Hofsteenge, J. (1989). The refined 1.9 Å crystal structure of human α-thrombin: interaction with D-Phe-Pro-Arg chloromethylketone and significance of the Tyr-Pro-Pro-Trp insertion segment. EMBO J. *8*, 3467–3475.

Bode, W., Brandstetter, H., Mather, T., and Stubbs, M.T. (1997). Comparative analysis of haemostatic proteinases: structural aspects of thrombin, factor Xa, factor IXa and protein C. Thromb. Haemost. *78*, 501–511.

Borgono, C.A. and Diamandis, E.P. (2004). The emerging roles of human tissue kallikreins in cancer. Nat. Rev. Cancer *4*, 876–890.

Borgoño, C.A., Gavigan, J.A., Alves, J., Bowles, B., Harris, J.L., Sotiropoulou, G., and Diamandis, E.P. (2007). Defining the extended substrate specificity of kallikrein 1-related peptidases. Biol. Chem. *388*, 1215–1225.

Brattsand, M. and Egelrud, T. (1999). Purification, molecular cloning, and expression of a human stratum corneum trypsin-like serine protease with possible function in desquamation. J. Biol. Chem. *274*, 30033–30040.

Brattsand, M., Stefansson, K., Lundh, C., Haasum, Y., and Egelrud, T. (2005). A proteolytic cascade of kallikreins in the stratum corneum. J. Invest. Dermatol. *124*, 198–203.

Caubet, C., Jonca, N., Brattsand, M., Guerrin, M., Bernard, D., Schmidt, R., Egelrud, T., Simon, M., and Serre, G. (2004). Degradation of corneodesmosome proteins by two serine proteases of the kallikrein family, SCTE/KLK5/hK5 and SCCE/KLK7/hK7. J. Invest. Dermatol. *122*, 1235–1244.

Chavanas, S., Bodemer, C., Rochat, A., Hamel-Teillac, D., Ali, M., Irvine, A.D., Bonafe, J.-L., Wilkinson, J., Taieb, A., Barrandon, Y., et al. (2000). Mutations in SPINK5, encoding a serine protease inhibitor, cause Netherton syndrome. Nat. Genet. *25*, 141–142.

Chen, Z. and Bode, W. (1983). Refined 2.5 Å X-ray crystal structure of the complex formed by porcine kallikrein A and the bovine pancreatic trypsin inhibitor. Crystallization, Patterson search, structure determination, refinement, structure and comparison with its components and with the bovine trypsin-pancreatic trypsin inhibitor complex. J. Mol. Biol. *164*, 283–311.

Clements, J., Hooper, J., Dong, Y., and Harvey, T. (2001). The expanded human kallikrein (KLK) gene family: genomic organisation, tissue-specific expression and potential functions. Biol. Chem. *382*, 5–14.

Clements, J.A., Hooper, J.D., Odorico, D.M., Dong, Y. (2004). The tissue kallikrein gene cluster. In: Handbook of Proteolytic Enzymes, A.J. Barrett, N.D. Rawlings, and J.F. Woessner, eds. (London, UK: Elsevier Academic Press), pp. 1569–1577.

Debela, M., Magdolen, V., Grimminger, V., Sommerhoff, C., Messerschmidt, A., Huber, R., Friedrich, R., Bode, W., and Goettig, P. (2006a). Crystal structures of human tissue kallikrein 4: activity modulation by a specific zinc binding site. J. Mol. Biol. *362*, 1094–1107.

Debela, M., Magdolen, V., Schechter, N., Valachova, M., Lottspeich, F., Craik, C.S., Choe, Y., Bode, W., and Goettig, P. (2006b). Specificity profiling of seven human tissue kallikreins reveals individual subsite preferences. J. Biol. Chem. *281*, 25678–25688.

Debela, M., Goettig, P., Magdolen, V., Huber, R., Schechter, N.M., and Bode, W. (2007a). Structural basis of the zinc inhibition of human tissue kallikrein 5. J. Mol. Biol. *373*, 1017–1031.

Debela, M., Hess, P., Magdolen, V., Schechter, N.M., Steiner, T., Huber, R., Bode, W., and Goettig, P. (2007b). Chymotryptic specificity determinants in the 1.0 Å structure of the zinc-inhibited human tissue kallikrein 7. Proc. Natl. Acad. Sci. USA *104*, 16086–16091.

Descargues, P., Deraison, C., Bonnart, C., Kreft, M., Kishibe, M., Ishida-Yamamoto, A., Elias, P., Barrandon, Y., Zambruno, G., Sonnenberg, A., and Hovnanian, A. (2005). Spink5-deficient mice mimic Netherton syndrome through degradation of desmoglein 1 by epidermal protease hyperactivity. Nat. Genet. *37*, 56–65.

Di Cera, E., Dang, Q.D., and Ayala, Y.M. (1997). Molecular mechanisms of thrombin function. Cell Mol. Life Sci. *53*, 701–730.

Diamandis, E.P., Yousef, G.M., Clements, J., Ashworth, L.K., Yoshida, S., Egelrud, T., Nelson, P.S., Shiosaka, S., Little, S., Lilja, H., et al. (2000). New nomenclature for the human tissue kallikrein gene family. Clin. Chem. *46*, 1855–1858.

Dong, Y., Kaushal, A., Brattsand, M., Nicklin, J., and Clements, J.A. (2003). Differential splicing of KLK5 and KLK7 in epithelial ovarian cancer produces novel variants with potential as cancer biomarkers. Clin. Cancer Res. *9*, 1710–1720.

Egelrud, T. (2004). Kallikrein 7. In: Handbook of Proteolytic Enzymes, A.J. Barrett, N.D. Rawlings, and J.F. Woessner, eds. (London, UK: Elsevier Academic Press), pp. 1556–1558.

Gros, P., Milder, F.J., and Janssen, B.J.C. (2008). Complement driven by conformational changes. Nat. Rev. Immunol. *8*, 48–58.

Hachem, J.P., Man, M.Q., Crumrine, D., Uchida, Y., Brown, B.E., Rogiers, V., Roseeuw, D., Feingold, K.R., and Elias, P.M. (2005). Sustained serine proteases activity by prolonged increase in pH leads to degradation of lipid processing enzymes and profound alterations of barrier function and stratum corneum integrity. J. Invest. Dermatol. *125*, 510–520.

Hart, P.S., Hart, T.C., Michalec, M.D., Ryu, O.H., Simmons, D., Hong, S., and Wright, J.T. (2004). Mutation in kallikrein 4 causes autosomal recessive hypomaturation amelogenesis imperfecta. J. Med. Genet. *41*, 545–549.

Harvey, T.J., Hooper, J.D., Myers, S.A., Stephenson, S.A., Ashworth, L.K., and Clements, J.A. (2000). Tissue-specific expression patterns and fine mapping of the human kallikrein (KLK) locus on proximal 19q13.4. J. Biol. Chem. *275*, 37397–37406.

Hoffman, B.R., Katsaros, D., Scorilas, A., Diamandis, P., Fracchioli, S., Rigault de la Longrais, I.A., Colgan, T., Puopolo, M., Giardina, G., et al. (2002). Immunofluorometric quantitation and histochemical localisation of kallikrein 6 protein in ovarian cancer tissue: a new independent unfavourable prognostic biomarker. Br. J. Cancer *87*, 763–771.

Huber, R. and Bode, W. (1978). Structural basis of the activation and action of trypsin. Acc. Chem. Res. *11*, 114–122.

Kim, H., Scorilas, A., Katsaros, D., Yousef, G.M., Massobrio, M., Fracchioli, S., Piccinno, R., Gordini, G., and Diamandis, E.P. (2001). Human kallikrein gene 5 (KLK5) expression is an indicator of poor prognosis in ovarian cancer. Br. J. Cancer *84*, 643–650.

Kurlender, L., Borgono, C., Michael, I.P., Obiezu, C., Elliott, M.B., Yousef, G.M., and Diamandis, E.P. (2005). A survey of alternative transcripts of human tissue kallikrein genes. Biochim. Biophys. Acta *1755*, 1–14.

Kyriakopoulou, L.G., Yousef, G.M., Scorilas, A., Katsaros, D., Massobrio, M., Fracchioli, S., and Diamandis, E.P. (2003). Prognostic value of quantitatively assessed KLK7 expression in ovarian cancer. Clin. Biochem. *36*, 135–143.

Laxmikanthan, G., Blaber, S.I., Bernett, M.J., Scarisbrick, I.A., Juliano, M.A., and Blaber, M. (2005). 1.70 A X-ray structure of human apo kallikrein 1: structural changes upon peptide inhibitor/substrate binding. Proteins *58*, 802–814.

Magklara, A., Mellati, A.A., Wasney, G.A., Little, S.P., Sotiropoulou, G., Becker, G.W., and Diamandis, E.P. (2003). Characterization of the enzymatic activity of human kallikrein 6: autoactivation, substrate specificity, and regulation by inhibitors. Biochem. Biophys. Res. Commun. *307*, 948–955.

Matsumura, M., Bhatt, A.S., Andress, D., Clegg, N., Takayama, T.K., Craik, C.S., and Nelson, P.S. (2005). Substrates of the prostate-specific serine protease prostase/KLK4 defined by positional-scanning peptide libraries. Prostate *62*, 1–13.

Menez, R., Michel, S., Muller, B.H., Bossus, M., Ducancel, F., Jolivet-Reynaud, C., and Stura, E.A. (2008). Crystal structure of a ternary complex between human prostate-specific antigen, its substrate acyl intermediate and an activating antibody. J. Mol. Biol. *376*, 1021–1033.

Michael, I.P., Pampalakis, G., Mikolajczyk, S.D., Malm, J., Sotiropoulou, G., and Diamandis, E.P. (2006). Human tissue kallikrein 5 is a member of a proteolytic cascade pathway involved in seminal clot liquefaction and potentially in prostate cancer progression. J. Biol. Chem. *281*, 12743–12750.

Michael, I.P., Sotiropoulou, G., Pampalakis, G., Magklara, A., Ghosh, M., Wasney, G., and Diamandis, E.P. (2005). Biochemical and enzymatic characterization of human kallikrein 5 (hK5), a novel serine protease potentially involved in cancer progression. J. Biol. Chem. *280*, 14628–14635.

Obiezu, C.V. and Diamandis, E.P. (2000). An alternatively spliced variant of KLK4 expressed in prostatic tissue. Clin. Biochem. *33*, 599–600.

Obiezu, C.V. and Diamandis, E.P. (2005). Human tissue kallikrein gene family: applications in cancer. Cancer Lett. *224*, 1–22.

Obiezu, C.V., Scorilas, A., Katsaros, D., Massobrio, M., Yousef, G.M., Fracchioli, S., Rigault de la Longrais, I.A., Arisio, R., and Diamandis, E.P. (2001). Higher human kallikrein gene 4 (KLK4) expression indicates poor prognosis of ovarian cancer patients. Clin. Cancer Res. *7*, 2380–2386.

Oikonomopoulou, K., Hansen, K.K., Saifeddine, M., Tea, I., Blaber, M., Blaber, S.I., Scarisbrick, I., Andrade-Gordon, P., Cottrell, G.S., Bunnett, N.W., et al. (2006a). Proteinase-activated receptors, targets for kallikrein signaling. J. Biol. Chem. *281*, 32095–32112.

Oikonomopoulou, K., Hansen, K.K., Saifeddine, M., Vergnolle, N., Tea, I., Blaber, M., Blaber, S.I., Scarisbrick, I., Diamandis, E.P., and Hollenberg, M.D. (2006b). Kallikrein-mediated cell signalling: targeting proteinase-activated receptors (PARs). Biol. Chem. *387*, 817–824.

Paliouras, M. and Diamandis, E.P. (2006). The kallikrein world: an update on the human tissue kallikreins. Biol. Chem. *387*, 643–652.

Paliouras, M. and Diamandis, E.P. (2007). Coordinated steroid hormone-dependent and independent expression of multiple kallikreins in breast cancer cell lines. Breast Cancer Res. Treat. *102*, 7–18.

Pampalakis, G. and Sotiropoulou, G. (2006). Multiple mechanisms underlie the aberrant expression of the human kallikrein 6 gene in breast cancer. Biol. Chem. *387*, 773–782.

Pampalakis, G. and Sotiropoulou, G. (2007). Tissue kallikrein proteolytic cascade pathways in normal physiology and cancer. Biochim. Biophys. Acta *1776*, 22–31.

Powers, J.C., Tanaka, T., Harper, J.W., Minematsu, Y., Barker, L., Lincoln, D., Crumley, K.V., Fraki, J.E., Schechter, N.M., Lazarus, G.G., et al. (1985). Mammalian chymotrypsin-like enzymes. Comparative reactivities of rat mast cell proteases, human and dog skin chymases, and human cathepsin G with peptide 4-nitroanilide substrates and with peptide chloromethyl ketone and sulfonyl fluoride inhibitors. Biochemistry *24*, 2048–2058.

Prezas, P., Arlt, M.J., Viktorov, P., Soosaipillai, A., Holzscheiter, L., Schmitt, M., Talieri, M., Diamandis, E.P., Kruger, A., and Magdolen, V. (2006). Overexpression of the human tissue kallikrein genes KLK4, 5, 6, and 7 increases the malignant phenotype of ovarian cancer cells. Biol. Chem. *387*, 807–811.

Schechter, I. and Berger, A. (1967). On the size of the active site in proteases. I. Papain. Biochem. Biophys. Res. Commun. *27*, 157–162.

Schechter, N.M., Choi, E.J., Wang, Z.M., Hanakawa, Y., Stanley, J.R., Kang, Y., Clayman, G.L., and Jayakumar, A. (2005). Inhibition of human kallikreins 5 and 7 by the serine protease inhibitor lympho-epithelial Kazal-type inhibitor (LEKTI). Biol. Chem. *386*, 1173–1184.

Shaw, J.L.V. and Diamandis, E.P. (2007). Distribution of 15 human kallikreins in tissues and biological fluids. Clin. Chem. *53*, 1423–1432.

Simmer, J.P. and Hu, J.C. (2002). Expression, structure, and function of enamel proteinases. Connect. Tissue Res. *43*, 441–449.

Simmer, J.P., Fukae, M., Tanabe, T., Yamakoshi, Y., Uchida, T., Xue, J., Margolis, H.C., Shimizu, M., DeHart, B.C., Hu, C.C., and Bartlett, J.D. (1998). Purification, characterization, and cloning of enamel matrix serine proteinase 1. J. Dent. Res. *77*, 377–386.

Skytt, A., Stromqvist, M., and Egelrud, T. (1995). Primary substrate specificity of recombinant human stratum corneum chymotryptic enzyme. Biochem. Biophys. Res. Commun. *211*, 586–589.

Stefansson, K., Brattsand, M., Roosterman, D., Kempkes, C., Bocheva, G., Steinhoff, M., and Egelrud, T. (2008). Activation of proteinase-activated receptor-2 by human kallikrein-related peptidases. J. Invest. Dermatol. *128*, 18–25.

Takayama, T.K., McMullen, B.A., Nelson, P.S., Matsumura, M., and Fujikawa, K. (2001). Characterization of hK4 (prostase), a prostate-specific serine protease: activation of the precursor of prostate-specific antigen (pro-PSA) and single-chain urokinase-type plasminogen activator and degradation of prostatic acid phosphatase. Biochemistry *40*, 15341–15348.

Tan, O.L., Whitbread, A.K., Clements, J.A., and Dong, Y. (2006). Kallikrein-related peptidase (KLK) family mRNA variants and protein isoforms in hormone-related cancers: do they have a function? Biol. Chem. *387*, 697–705.

Wright, J.T., Hart, P.S., Aldred, M.J., Seow, K., Crawford, P.J., Hong, S.P., Gibson, C.W., and Hart, T.C. (2003). Relationship of phenotype and genotype in X-linked amelogenesis imperfecta. Connect. Tissue Res. *44*, 72–78.

Yamaguchi, N. (2004). Neurosin or human kallikrein 6. In: Handbook of Proteolytic Enzymes, A.J. Barrett, N.D. Rawlings, and J.F. Woessner, eds. (London, UK: Elsevier Academic Press), pp. 1585–1587.

Yamakoshi, Y., Hu, J.C., Fukae, M., Yamakoshi, F., and Simmer, J.P. (2006). How do enamelysin and kallikrein 4 process the 32-kDa enamelin? Eur. J. Oral. Sci. *114* (Suppl. 1), 45–51; discussion 93–45, 379–380.

Yamasaki, K., Schauber, J., Coda, A., Lin, H., Dorschner, R.A., Schechter, N.M., Bonnart, C., Descargues, P., Hovnanian, A., and Gallo, R.L. (2006). Kallikrein-mediated proteolysis regulates the antimicrobial effects of cathelicidins in skin. FASEB J. *20*, 2068–2080.

Yoon, H., Laxmikanthan, G., Lee, J., Blaber, S.I., Rodriguez, A., Kogot, J.M., Scarisbrick, I.A., and Blaber, M. (2007). Activation profiles and regulatory cascades of the human kallikrein-related peptidases. J. Biol. Chem. *282*, 31852–31864.

Yousef, G.M. and Diamandis, E.P. (2001). The new human tissue kallikrein gene family: structure, function, and association to disease. Endocr. Rev. *22*, 184–204.

Yousef, G.M. and Diamandis, E.P. (2002). Human tissue kallikreins: a new enzymatic cascade pathway? Biol. Chem. *383*, 1045–1057.

Yousef, G.M. and Diamandis, E.P. (2003). An overview of the kallikrein gene families in humans and other species: emerging candidate tumour markers. Clin. Biochem. *36*, 443–452.

Yousef, G.M., Luo, L.Y., and Diamandis, E.P. (1999). Identification of novel human kallikrein-like genes on chromosome 19q13.3-q13.4. Anticancer Res. *19*, 2843–2852.

Yousef, G.M., Chang, A., Scorilas, A., and Diamandis, E.P. (2000). Genomic organization of the human kallikrein gene family on chromosome 19q13.3-q13.4. Biochem. Biophys. Res. Commun. *276*, 125–133.

Yousef, G.M., Whitea, N.M.A., Kurlender, L., Michael, I., Memari, N., Robba, J.-D., Katsaros, D., Stephane, C., Junge, K., and Diamandis, E.P. (2004). The kallikrein gene 5 splice variant 2 Is a new biomarker for breast and ovarian cancer. Tumor Biol. *25*, 221–227.